Voltage Dependence of the Apparent Affinity for External Na^+ of the Backward-running Sodium Pump

Paul De Weer, David C. Gadsby, and R.F. Rakowski

From the Marine Biological Laboratory, Woods Hole, Massachusetts 02543

ABSTRACT The steady-state voltage and $[Na^+]_o$ dependence of the electrogenic sodium pump was investigated in voltage-clamped internally dialyzed giant axons of the squid, *Loligo pealei*, under conditions that promote the backward-running mode (K^+-free seawater; ATP- and Na^+-free internal solution containing ADP and orthophosphate). The ratio of pump-mediated $^{42}K^+$ efflux to reverse pump current, I_{pump} (both defined by sensitivity to dihydrodigitoxigenin, H_2DTG), scaled by Faraday's constant, was -1.5 ± 0.4 ($n = 5$; expected ratio for 2 K^+/3 Na^+ stoichiometry is -2.0). Steady-state reverse pump current-voltage (I_{pump}-V) relationships were obtained either from the shifts in holding current after repeated exposures of an axon clamped at various V_m to H_2DTG or from the difference between membrane I-V relationships obtained by imposing V_m staircases in the presence or absence of H_2DTG. With the second method, we also investigated the influence of $[Na^+]_o$ (up to 800 mM, for which hypertonic solutions were used) on the steady-state reverse I_{pump}-V relationship. The reverse I_{pump}-V relationship is sigmoid, I_{pump} saturating at large negative V_m, and each doubling of $[Na^+]_o$ causes a fixed (29 mV) rightward parallel shift along the voltage axis of this Boltzmann partition function (apparent valence $z = 0.80$). These characteristics mirror those of steady-state $^{22}Na^+$ efflux during electroneutral Na^+/Na^+ exchange, and follow without additional postulates from the same simple high field access channel model (Gadsby, D.C., R.F. Rakowski, and P. De Weer, 1993. *Science.* 260: 100–103). This model predicts valence $z = n\lambda$, where n (1.33 ± 0.05) is the Hill coefficient of Na binding, and λ (0.61 ± 0.03) is the fraction of the membrane electric field traversed by Na ions reaching their binding site. More elaborate alternative models can accommodate all the steady-state features of the reverse pumping and electroneutral Na^+/Na^+ exchange modes only with additional assumptions that render them less likely.

KEY WORDS: Na,K-ATPase • electrogenicity • active transport • kinetics • modeling

INTRODUCTION

The electrogenic sodium pump or Na,K-ATPase exports three Na ions and imports two K ions for each molecule of ATP hydrolyzed. According to the generally accepted Albers-Post model (Albers, 1967; Post et al., 1969; also see Fig. 8) the Na,K-ATPase undergoes a sequence of conformational changes driven by phosphorylation/dephosphorylation reactions, during which the pump's binding sites for Na^+ and K^+ alternately face the intracellular and extracellular sides of the cell membrane. The sodium pump molecule belongs to the superfamily of P-type ATPases (Axelsen and Palmgren, 1998), so named after the phosphorylation and dephosphorylation they undergo during their enzymatic cycle. The only high resolution P-type ATPase structure published to date is that for the Ca-ATPase of the sarcoplasmic reticulum (Toyoshima et al., 2000). In the absence of a high resolution structure for the sodium pump, it is possible to formulate structural constraints from a detailed analysis of the pump's kinetics. Provided its stoichiometry remains fixed, a sensitive measure of an electrogenic transporter's steady-state turnover rate is the transmembrane current it generates.

Information on charge-translocating steps in a transporter's reaction cycle can be obtained from the voltage dependence of the turnover rate of its various modes of operation (for reviews see De Weer et al., 1988, 2000; Apell, 1989; Läuger, 1991a,b; Rakowski et al., 1997b). Transient sodium pump currents elicited by [ATP] or voltage jumps in the absence of external K^+ suggest that at least one charge-moving step accompanies deocclusion/release of Na ions to the exterior. Three of the pump's modes of operation involve Na^+ translocation: forward pumping, ADP-dependent Na^+/Na^+ exchange, and reverse pumping. The voltage and $[Na^+]_o$ dependence of the former two have been examined so far. Steady-state pump current-voltage (I_{pump}-V) relationships have been obtained for the forward-running mode of the Na/K pump in cardiac ventricular myocytes (Gadsby et al., 1985; Gadsby and Nakao, 1989; Nakao and Gadsby, 1989; Peluffo and Berlin, 1997), cardiac Purkinje cells (Glitsch et al., 1989; Bielen et al.,

The present address of Dr. Gadsby is Laboratory of Cardiac/Membrane Physiology, The Rockefeller University, 1230 York Avenue, New York, NY 10021. The present address of Dr. Rakowski is Department of Biological Sciences, Ohio University, Irvine Hall, Athens, OH 45701.

Address correspondence to Dr. Paul De Weer, Department of Physiology, University of Pennsylvania School of Medicine, Philadelphia, PA 19104-6085. Fax (215) 573-5851; E-mail: deweer@mail.med.upenn.edu

1991), *Xenopus* oocytes (Lafaire and Schwarz, 1986; Horisberger et al., 1991; Rakowski and Paxson, 1988; Rakowski et al., 1991; Sagar and Rakowski, 1994), HeLa (Argüello et al., 1996) or HEK293 (Kockskämper et al., 1997) cells expressing recombinant pump molecules, and squid giant axons (Rakowski et al., 1989). In all preparations, at near-saturating intracellular sodium ($[Na^+]_i$) and extracellular potassium concentrations ($[K^+]_o$), the I-V relationship of the forward-running pump at high extracellular sodium concentration ($[Na^+]_o$) is approximately sigmoid, approaching a plateau or shallow positive slope at large positive potentials and tending towards zero at very negative potentials. In the absence of extracellular Na^+, however, the pump current at saturating $[K^+]_o$ is nearly voltage-independent over the accessible voltage range. In squid axons, the pump's coupling ratio in the forward transport mode is 3 Na^+/2 K^+ and independent of $[Na^+]_o$ or membrane potential (Rakowski et al., 1989). Moreover, in both high and low $[Na^+]_o$ media, membrane potential affects pump current (i.e., net transport) and radiotracer Na^+ efflux (i.e., unidirectional transport) in closely parallel fashion, signifying that the marked effects of $[Na^+]_o$ on the I-V relationship of the pump in the forward mode reflect selective voltage-dependent slowing, by $[Na^+]_o$, of forward pump turnover and not, for example, stimulation of reverse transport.

Much evidence shows that extracellular Na^+ and K^+ both interact with the Na/K pump at sites within the membrane's electric field (Läuger, 1991a,b). Rakowski et al. (1991), Stürmer et al. (1991), and Bielen et al. (1993) found that the apparent affinity for activation of the forward-running pump by K^+ is enhanced by hyperpolarization. Although this might reflect voltage dependence of any step in the K^+ translocation pathway, the observation that K^+ translocation is electrically silent at saturating $[K^+]_o$ (Goldshlegger et al., 1987; Bahinski et al., 1988; Stürmer et al., 1989) strongly suggests that K^+ binding is voltage-dependent and, hence, that extracellular K ions might reach their binding sites through an access channel. A more direct argument for a high field access/release channel between ion binding sites in the pump and the external medium is found in our analysis, in squid giant axons, of the voltage dependence of the ADP-requiring electroneutral Na^+/Na^+ exchange mode in K^+-free media (Gadsby et al., 1993). The rate of this Na^+/Na^+ exchange flux ($\Phi_{Na/Na}$) declines at positive potentials, but, upon membrane hyperpolarization rises along an apparently saturating sigmoid curve. Furthermore, activation of Na^+/Na^+ exchange by Na_o^+ and by hyperpolarization are kinetically equivalent (Mitchell, 1969) so that the flux-voltage ($\Phi_{Na/Na}$-V) curve is simply shifted laterally when $[Na^+]_o$ is altered. Both characteristics point to a voltage sensitivity related to the external Na^+ rebinding step, which therefore must be influenced by the membrane field (Gadsby et al., 1993).

A third mode of operation of the sodium pump, besides electrogenic forward Na^+/K^+ transport and electroneutral Na^+/Na^+ exchange, is electrogenic K^+/Na^+ transport in which the cycle runs backwards to generate both ATP (Garrahan and Glynn, 1967; Chmouliovsky, 1970; Lew et al., 1970) and an inward current (De Weer and Rakowski, 1984; Bahinski et al., 1988; Efthymiadis and Schwarz, 1991). Because all Na^+-translocating modes of operation of the pump share one or more reaction steps, it is important to establish the extent to which these common steps bring about common overall kinetic behavior, in particular, voltage sensitivity. We investigate here the voltage and $[Na^+]_o$ dependence of backward-running sodium pump current in voltage-clamped internally dialyzed squid giant axons. We show that, as is the case for electroneutral Na^+/Na^+ exchange, the voltage dependence of electrogenic backward pumping is sigmoid with the current apparently saturating at large negative potentials, and that alterations in $[Na^+]_o$ cause simple parallel shifts of this curve along the voltage axis. The high field access channel model we proposed for electroneutral Na^+/Na^+ exchange (Gadsby et al., 1993) predicts such behavior.

MATERIALS AND METHODS

Voltage Clamp and Internal Dialysis

Membrane current and unidirectional $^{42}K^+$ tracer efflux were measured in voltage-clamped internally dialyzed giant axons of the squid, *Loligo pealei,* using methods previously described (Rakowski et al., 1989). In brief, a porous, 160-μm-diam cellulose acetate capillary was inserted through one cannulated end of the axon while a glass voltage-measuring electrode and piggyback blackened platinum wire (each ~75 μm in diameter) were inserted through the other end. A conventional voltage clamp circuit measured membrane current, and two ancillary voltage clamp circuits prevented longitudinal stray current flow between the center pool and adjacent guard pools. The cytoplasmic composition was maintained and, in some cases, $^{42}K^+$ was introduced inside the axon by perfusing the porous intracellular capillary (1.4 μl/min) with appropriate solutions. To measure $^{42}K^+$ efflux, the artificial seawater superfusing (2 ml/min) the axon in the center pool was collected in scintillation counting vials. Initial experiments were carried out near 17°C; but, to increase sodium pump turnover rate and hence signal magnitude, the temperature was raised to ~22°C in later experiments (see Figs. 4 and 7). A 30–60 min period of dialysis (to allow for equilibration) preceded data collection in all experiments.

Solutions

External solutions were K^+-free artificial seawater typically containing (in mM): 400 Na isethionate, 75 Ca sulfamate, 5 Tris HEPES, pH 7.7, 1 3,4-diaminopyridine (DAP), 0.1 Tris EDTA, and 0.2 μM tetrodotoxin (TTX). In 200 mM-Na^+ seawater *N*-methyl-D-glucamine (NMG) sulfamate replaced half of the Na isethionate. In some early experiments, chloride replaced the isethionate and sulfamate. The internal dialysis solutions were Na^+-free and typically contained (in mM): ~160 K^+, 100 glycine, 50 phenylpro-

pyltriethylammonium (PPTEA) sulfate, 2.5 BAPTA, 40 Mg HEPES, 5 dithiothreitol, 25 ADP, and 25 orthophosphate, pH ~7.5; the principal anion was HEPES. In some early experiments, EGTA replaced BAPTA, $MgSO_4$ or $MgCl_2$ replaced Mg HEPES, and 20–25 mM L-arginine (a substrate for arginine kinase) sulfate or chloride, 1–2.5 mM Li_5-diadenosine pentaphosphate (an inhibitor of adenylate kinase), and 50–100 μM Na atractyloside (an inhibitor of mitochondrial ATP/ADP transfer) were added to minimize ATP accumulation within the axon. The osmolality of these internal solutions was 930–940 mOsm/kg, and that of the external solutions was 920–930 mOsm/kg. To extend the experimental $[Na^+]_o$ range, hypertonic (1,780–1,790 mOsm/kg) internal and external solutions were used in some cases. In hypertonic dialysis fluid, 130 mM NMG HEPES replaced glycine. One hypertonic artificial seawater matched the typical composition above except that it contained 800 mM Na isethionate, and the other contained 800 mM NMG sulfamate instead. Intermediate (200 and 400 mM) Na concentrations were obtained by mixing.

External TTX and DAP, and internal PPTEA, minimized nonpump Na and K channel currents (Rakowski et al., 1989), and internal BAPTA or EGTA kept internal $[Ca^{2+}]$ low to suppress Na^+/Ca^{2+} exchange (DiPolo and Beaugé, 1987). The external K^+- and internal Na^+- and ATP-free conditions were designed to prevent forward, and promote reverse, Na/K pump cycling. To reduce membrane conductance in the end pools, those regions were bathed in K^+-free, Na^+-free seawater (NMG sulfamate replaced Na isethionate) containing 100 μM dihydrodigitoxigenin (H_2DTG)[1] in addition to TTX and DAP. Na/K pump-mediated current and $^{42}K^+$ efflux were defined as those components abolished by sudden introduction of 10 or 100 μM H_2DTG into the center pool (100 μM was used in all experiments in which $[Na^+]_o$ was varied, and in many at 400 mM $[Na^+]_o$). The pump is inhibited ~90% by 10 μM H_2DTG in 400 mM–Na^+, K^+-free seawater (Gadsby et al., 1993) and ~94% by 100 μM H_2DTG in Na^+-free seawater (Rakowski et al., 1989). H_2DTG was added from a 100-mM stock solution in DMSO whose final concentration (≤0.1% vol/vol) did not affect the membrane current under our conditions (see Fig. 5 A). Ouabain was used at 100 μM, from a 10-mM stock solution in the appropriate artificial seawater. DAP was added directly to artificial seawater, and TTX from a 1-mM aqueous stock.

Correction for Baseline Drift

In two instances the shapes of several I-V plots obtained under different conditions and/or from different axons needed to be rigorously compared (two experiments on a single axon are compared in Fig. 6 C, and numerous experiments on two dozen axons are compared in Fig. 7, A and B). To that end, it was necessary to correct each individual "raw" H_2DTG (or ouabain) difference I-V curve for any inadvertently included spontaneous baseline conductance drift. Baseline drift was estimated from "time only" differences (typically two before, and two after, exposure to the pump blocker) between consecutive I-V plots recorded at time intervals matching that between the I-V plots obtained just before and shortly after addition of the pump blocker (illustrated in Fig. 4). To avoid the sampling noise that would result from point-by-point correction, the "time only" difference I-V plots were individually fit with second-degree polynomials, a time-weighted average of which was then subtracted from the raw signal difference to yield the drift-corrected H_2DTG-sensitive I-V plot. To obviate time weighting, the six experimental I-V records were generally (as in Fig. 4) evenly spaced. The drift correction was usually small (≤6% of I_{pump} at −60 mV in most axons.)

[1]*Abbreviation used in this paper:* H_2DTG, dihydrodigitoxigenin.

Global Least-Squares Fit of Access Channel Model to the Data of Fig. 7

Our access-channel model (see DISCUSSION) yields an S-shaped expression for the voltage and $[Na^+]_o$ dependent reverse pump current of the form:

$$I_{pump} = \frac{I_{pump}^{max}}{1 + \left(\frac{K_{0.5}^0}{[Na^+]_o} \cdot e^{V_m \frac{\lambda F}{RT}} \right)^n},$$

(where V_m is membrane potential and F, R, and T have their usual meaning), such that reverse I_{pump} vanishes at extreme positive potentials and reaches I_{pump}^{max} at extreme negative potentials. This expression can be interpreted either as a Boltzmann partition equation with $[Na^+]_o$-dependent midpoint or as a Hill approximation with fixed Hill coefficient n but voltage-dependent affinity for external Na^+. $K_{0.5}^0$ is the apparent dissociation constant of a Na^+-binding site at the bottom of an access channel in the absence of transmembrane field, and λ is the access channel's depth as a fraction of electrical distance across the membrane, measured from the external solution.

To combine and compare multiple data sets from different axons (see Fig. 7), the following procedure was adopted. All I-V plots, individually corrected for baseline drift as described, were simultaneously fit, in a global least-squares procedure (Simchowitz et al., 1986), with Boltzmann equations of the above form, appropriate for the temperature at which each experiment had been carried out. The global fit generated two adjustable parameters for each individual I-V plot: a scaling variable I_{pump}^{max} and any nonzero offset at large positive potentials (not shown in the above equation, but see RESULTS). In addition, the global least-squares fit estimated the following adjustable parameters: (1) an apparent access channel depth (or fraction of the field traversed) (λ) common to all experiments; (2) a Hill coefficient n common to all experiments; and (3) two values for the apparent Na affinity in the absence of membrane potential ($K_{0.5}^0$): one value shared by all normotonic experiments (see Fig. 7 A) and another shared by all hypertonic experiments (see Fig. 7 B). All theoretical curves in Fig. 7 are drawn for 22°C (where RT/F = 25.34 mV) with these common parameters, and with normalized $I_{pump}^{max} = -1$ and no offset at positive voltages. The drift-corrected data were offset to zero at large positive voltages, normalized to −1 at large negative voltages, grouped by experimental protocol, and averaged. Symbols represent averages ± SEM. Lognormal statistics were used to calculate the standard error of ratios.

RESULTS

Reverse Pump Stoichiometry: Simultaneous Measurements of H_2DTG-sensitive Current and $^{42}K^+$ Efflux

Fig. 1 shows representative results from one of five axons engaged in reverse pumping in which H_2DTG-sensitive current and $^{42}K^+$ efflux were measured simultaneously at −60 mV. Since H_2DTG is a specific Na/K pump inhibitor without additional effects (but see below) the small H_2DTG-induced outward shift of the holding current ($\Delta I = 0.055$ μA cm^{-2} in Fig. 1 A) must reflect abolition of the inward current generated by the backward-running Na/K pump. H_2DTG washout allows repetition of this type of experiment. The mean ΔI of three successive trials on the axon of Fig. 1 A was 0.056 ± 0.002 μA cm^{-2}. Fig. 1 B shows the average of

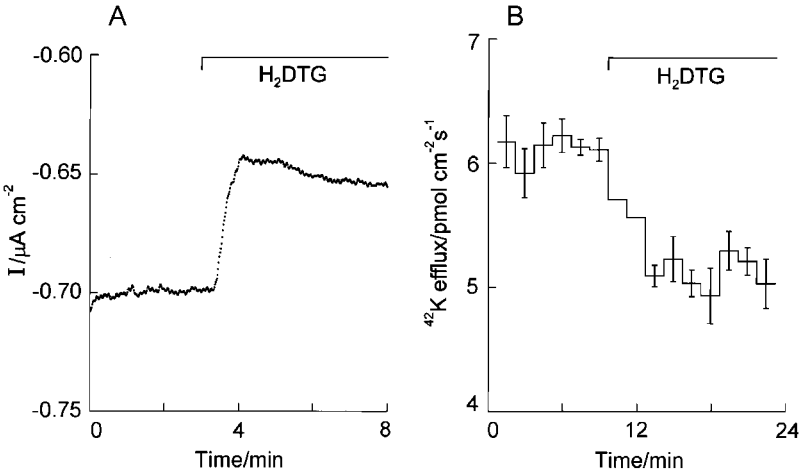

FIGURE 1. Comparison of the shift in holding current (A, single episode) and drop in $^{42}K^+$ efflux (B, average of three) produced by 100 μM H_2DTG in the same axon (25 min between exposures to permit inhibitor washout). (B) Ordinate is scaled to that of A by 2× Faraday's constant; a deflection of similar size produced by H_2DTG in A and B, therefore, signifies that one net charge moves inward per two K ions extruded, as expected for a 2 K^+/3 Na^+ pump cycle extruding K^+ and taking up Na^+. The longer time scale in B reflects mixing delays in the $^{42}K^+$ collection system. Axon internally dialyzed with Na^+-free, 160 mM-K (radiolabeled) solution and bathed in 400 mM-Na^+, K^+-free artificial seawater. Temperature, 17.9°C.

the corresponding three $^{42}K^+$ efflux determinations; mean H_2DTG-sensitive K efflux ($-\Delta\Phi$) was 1.04 ± 0.07 pmol cm^{-2} s^{-1} in this axon, yielding a value of 1.79 ± 0.22 for the ratio $-F\Delta\Phi/\Delta$ (where F is Faraday's constant), which is compatible with the value of 2.0 expected for 2 K^+/3 Na^+ transport stoichiometry. The mean values of ΔI and ΔΦ for all five axons were 0.106 ± 0.011 μA cm^{-2} (n = 18) and −1.46 ± 0.19 pmol cm^{-2} s^{-1} (n = 16). The (geometric) mean of the individual $-F\Delta\Phi/\Delta I$ ratios was 1.5 ± 0.4, not significantly ($P > 0.2$) different from 2.0. The correspondence of H_2DTG-sensitive current and flux argues that both reflect backward cycling of the Na/K pump.

Membrane Potential Effect on Reverse Pump Current

We used two procedures to estimate the voltage dependence of reverse pump current magnitude. The first determined the magnitude of H_2DTG-sensitive current at various holding potentials by repeated exposures of an axon to H_2DTG with intervening periods of washout. Fig. 2 shows successive H_2DTG-induced holding current shifts in a single axon. The records in the first column (at the reference holding potential of −40 mV) show a steady decline of reverse pump current magnitude with time. The ΔI measurements at other holding potentials, therefore, were corrected for this rundown by exponential interpolation (extrapolation for final measurement). The H_2DTG-induced ΔI is large at negative potentials, negligible at about +10 mV, and reversed at +30 mV. Data from 14 axons (including that of Fig. 2) are summarized in Fig. 3 A, which plots the magnitude of the abolished backward-running pump current. In six of these axons, bracketed data allowed correction for rundown and normalization to the interpolated magnitude of the H_2DTG-induced ΔI at −40 mV (Fig. 3 B). The results show that reverse pump current magnitude increases monotonically with hyperpolarization throughout the voltage range examined. The small outward current at +30 mV is probably caused by small variations of [K^+] in the extracellular space, as will be discussed later.

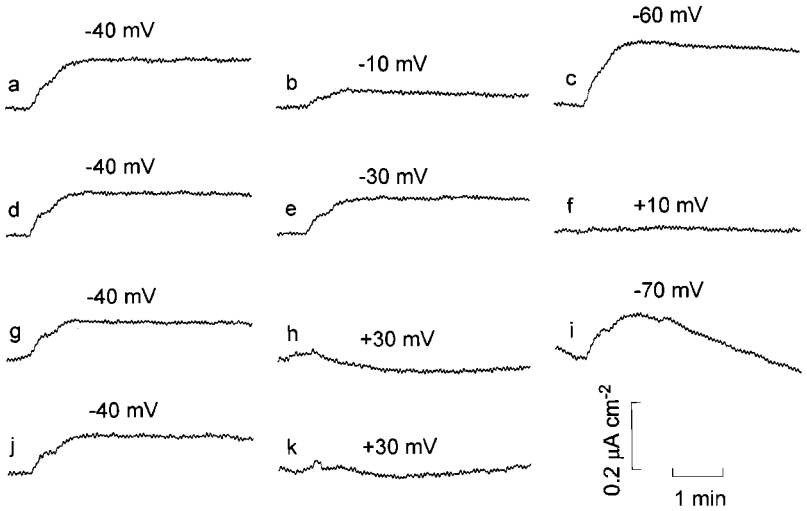

FIGURE 2. Changes in holding current (ΔI) produced by 7-min exposures to 10 μM H_2DTG, each followed by a 30-min washout, made in the alphabetical sequence shown. The holding potential was reset during washout, ensuring ≥10 min at each new potential before fresh H_2DTG addition. The ΔI is generally outward, which is consistent with removal of an inwardly directed Na/K pump current; small inward shifts were seen at +30 mV (h and k). The response magnitude at −40 mV declined progressively (a, d, g, and j) during the experiment. Axon perfused with 160 mM-K, Na^+-free solution and bathed in 400 mM-Na^+, K^+-free solution. Temperature, 17.4°C.

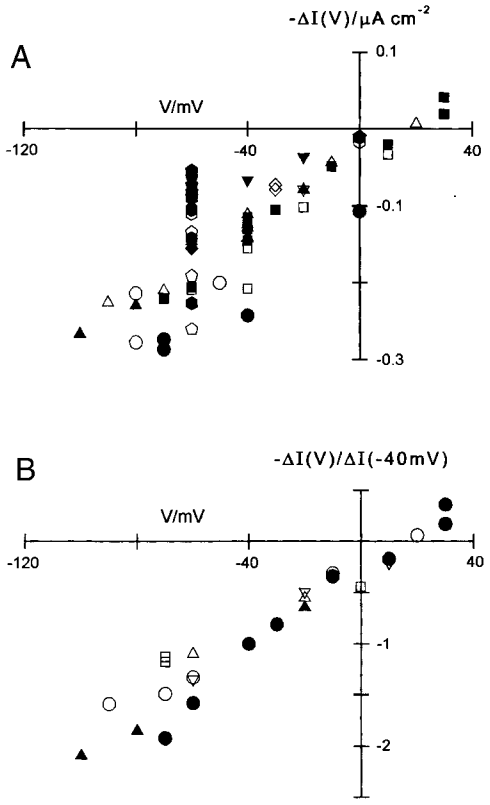

FIGURE 3. Current-voltage relationship of the backward-running Na/K pump constructed from many shifts in holding current (ΔI) produced by 10 μM H_2DTG. (A) H_2DTG-sensitive currents (−ΔI) at various membrane potentials in 14 axons (different symbols); not corrected for rundown. (B) Normalized data. All the data from six axons for which the rundown rate could be established by inter- or extrapolation are plotted relative to measurements at −40 mV. Closed circles are from the axon of Fig. 2. $[Na^+]_o$ was 400 mM. Temperature range, 17.3–17.6°C.

Reverse Pump Current-Voltage Relationship

In the second method, illustrated in Fig. 4, we recorded entire steady-state I-V curves in the absence and presence of H_2DTG (or ouabain), and obtained the reverse pump I-V relation by difference, subject to correction for any baseline drift. This method, though unsuited for simultaneous measurement of $^{42}K^+$ efflux, more accurately renders the shape of the I-V relationship and (being rapid) is much less affected by rundown. Fig. 4 A shows a sequence (a–f) of six identical 48-step down-up-down membrane potential staircases (1 s per 5-mV step) imposed from a holding potential of −30 mV, before and during exposure to 100 μM H_2DTG. Fig. 4 B shows the resulting changes in membrane current, as well as the outward shift upon application of H_2DTG (between c and d) reflecting abolition of inwardly directed reverse pump current. The repeated I-V measurements allowed accurate assessment of any spontaneous drift in the shape of the membrane I-V curve before and/or after H_2DTG addition.

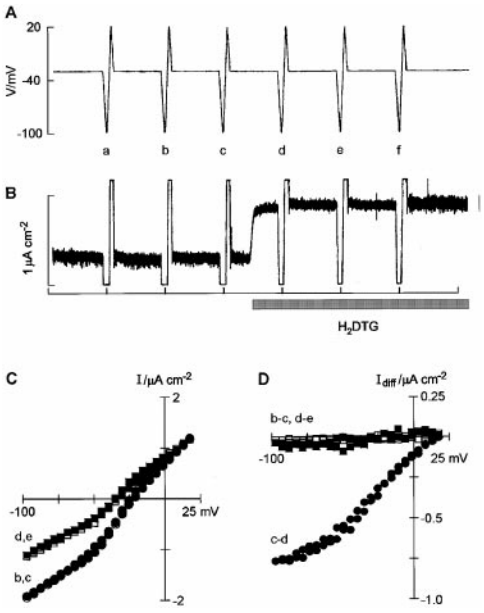

FIGURE 4. I-V relationship of the backward-running Na/K pump obtained from the difference between steady-state I-V curves before and during application of 100 μM H_2DTG, with provision for correction for spontaneous baseline drift. (A) A down-up-down voltage staircase, from −30 to −100 mV, then to +20 mV, and back to −30 mV, was applied at 5-min intervals before (a–c) and after (d–f) addition of H_2DTG. (B) Current shifts upon imposition of voltage staircases (partially off-scale in this analogue chart record, but within range of the digital sampling system) or application of H_2DTG. Tic marks are 5 min apart. (C) Steady-state I-V relationships obtained immediately before ([closed circles] b and [open circles] c) and shortly after ([closed squares] d and [open squares] e) application of H_2DTG. The two consecutive I-V relationships in each condition are nearly superimposable, and none of the curves shows significant hysteresis. (D) Difference I-V relationships. Closed circles are point-by-point differences between I-V curves (from panel C) obtained just before (c) and shortly after (d) application of H_2DTG, and represent an approximate (raw) H_2DTG-sensitive I-V plot still uncorrected for any spontaneous baseline drift during the 5-min interval between c and d. Estimates for such drift with time are computed as the difference between successive pairs of I-V curves taken before ([open squares] b and c) and during ([closed squares] d and e) the application of H_2DTG. For clarity, the two additional estimates available for baseline drift correction (a and b and e and f) are not shown. $[Na^+]_o$ was 400 mM. Temperature, 21.5°C.

Fig. 4 C shows four (of the six) corresponding steady-state membrane I-V relationships, two (b and c; circles) before and two (d and e; squares) during exposure to H_2DTG, obtained by plotting the current recorded near the end of each 1-s staircase step against step voltage. The measured currents reflect a true steady state as there was negligible hysteresis in the I-V plots, the same steady-state current being obtained at a given voltage during ascending and descending limbs of the staircase. The overlapping of open and filled symbols in Fig. 4 C indicates only modest drift with time. The difference (Fig. 4 D, c and d; closed circles) between

records just before (c) and shortly after (d) H_2DTG addition gives a raw H_2DTG-sensitive I-V plot, so qualified because it is not corrected for any unrelated, spontaneous baseline drift that occurred during the 5-min interval between c and d. Even without baseline drift correction, the voltage dependence of H_2DTG-sensitive current is clearly sigmoid, with inward current apparently saturating at large negative potentials.

Four estimates of how much the baseline drifted during an equivalent time interval are given by difference I-V relationships obtained in the absence (a minus b and b minus c) and presence (d minus e and e minus f) of H_2DTG; one of each is shown in Fig. 4 D. The raw H_2DTG-sensitive I-V plot, if necessary (see MATERIALS AND METHODS), can be corrected for this – here negligibly small – baseline drift. For any V_m, the drift-corrected H_2DTG-sensitive current is given by the distance between the raw H_2DTG-sensitive plot and the background drift plot.

Evidence that H_2DTG-induced Shifts in Holding Current Represent Na/K Pump Current

We have previously established (Rakowski et al., 1989) that, in squid axons, H_2DTG-sensitive current may be equated with Na/K pump current under forward-running pump conditions. Fig. 5 demonstrates the same for the reverse pumping mode. Control application (Fig. 5 A) of 0.1% DMSO, the solvent we used for H_2DTG, caused no change in membrane currents in the presence of 100 μM ouabain (to inhibit the pump). DMSO also caused no change in the absence of ouabain (not shown). Application of 100 μM H_2DTG plus 0.1% DMSO in the presence of ouabain (Fig. 5 B) also had no perceptible effect at any voltage. These results confirm that neither H_2DTG nor DMSO has any electrophysiologically discernible effect on nonpump currents. Other tests (not shown) verified that 100 μM ouabain had no measurable effect on axons already exposed to 100 μM H_2DTG.

As in the case of forward Na/K pump current (Gadsby and Nakao, 1989; Rakowski et al., 1989), if H_2DTG-sensitive current is to be equated with current generated directly by reverse pumping, it must be shown that any changes in K^+-sensitive electrodiffusional currents are negligible. Indeed, reverse operation of the Na/K pump (in nominally K^+-free seawater) is expected to establish, in the restricted-diffusion space between axolemma and Schwann cells, a finite $[K^+]$ which should fall back to zero once the pump is arrested with ouabain or H_2DTG. These activity-dependent $[K^+]_o$ variations, estimated to reach 1 mM in the case of forward pumping (Rakowski et al., 1989), are likely to be smaller for the slower reverse pump. Fig. 5 C shows a stringent test of the effectiveness of our block of K^+-sensitive nonpump current, the mean membrane current shift (seven tests on three

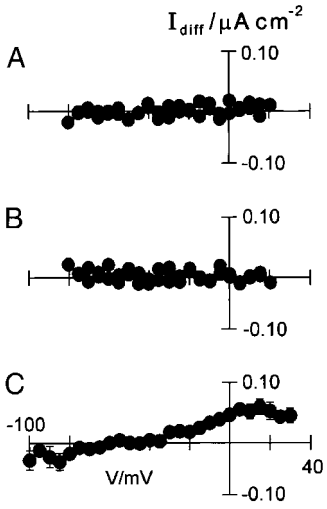

FIGURE 5. Control experiments. (A) Lack of effect of DMSO. Difference currents shown obtained by subtracting I-V data in the presence of 0.1% DMSO from data obtained before its application. The axon previously had been exposed to 100 μM ouabain. (B) Lack of effect of H_2DTG on membrane current in an axon already exposed to 100 μM ouabain. The difference currents shown were obtained by subtracting data collected during exposure to 100 μM H_2DTG from data before its application. No correction for baseline drift, which was imperceptible in these axons, was applied in A or B; the raw difference records are shown. (C) K^+-sensitive current not blocked by 50 mM internal PPTEA and 1 mM external DAP. An estimate of the maximum error that could result from local $[K^+]_o$ changes on stopping the Na/K pump is obtained by making deliberate $[K^+]_o$ changes in the presence of 100 μM ouabain. The I-V data obtained in K^+-free solution were subtracted from those obtained in the presence of 10 mM K^+ and corrected for baseline drift. The average values ± SEM (seven measurements on three axons) of the residual K^+-sensitive current are shown. Temperature (all three axons), 17.8°C.

axons) caused by switching from K^+-free solution to a 10-mM K^+ solution in the presence of 100 μM ouabain and 1 mM DAP externally and of 50 mM PPTEA internally. Since this residual current is presumably carried by inward-rectifier K channels that are sensitive to extracellular K^+, it will decline as $[K^+]_o$ drops when reverse pumping is stopped and, thus, contribute to the measured H_2DTG-sensitive current. Such nonpump, yet indirectly H_2DTG-sensitive, current component likely accounts for the small outward H_2DTG-sensitive current seen at positive potentials (Figs. 2, 3, and 6 B) despite the nominal absence of extracellular K^+. Thus, the data in Figs. 4 and 5 show that H_2DTG-sensitive current may be equated with reverse pump current under our experimental conditions. Possible inclusion of a small K^+-sensitive, nonpump current (a minor fraction of that obtained with 10 mM K in Fig. 5 C) masquerading as reverse pump current, does not materially affect our conclusions.

H_2DTG- and Ouabain-sensitive Currents

Current-voltage relationships of the backward-running pump obtained by H_2DTG or ouabain inhibition are compared in Fig. 6. Fig. 6 A shows (closed circles) the mean raw H_2DTG difference I-V relationship obtained from seven measurements on four axons. (The absolute current magnitudes were sufficiently similar to warrant simple averaging without normalization.) Open circles show the average ± SEM of the corresponding seven

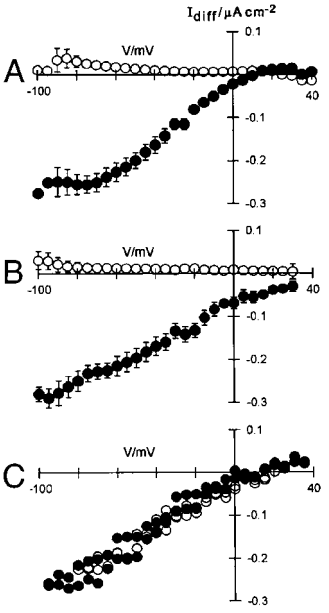

FIGURE 6. I-V relationship of the backward-running Na/K pump obtained by H_2DTG or ouabain addition. (A) Solid symbols represent the mean value of H_2DTG-sensitive current (uncorrected for drift) obtained from seven measurements on four axons. The open symbols represent the mean I-V drift that occurred during the same interval of time (~5 min) that was needed to record the H_2DTG difference I-V data. (B) Closed symbols represent the mean value of ouabain-sensitive current obtained from four axons. Open symbols represent the mean I-V drift occurring during a time interval similar to that required to record the ouabain difference I-V data. (C) Comparison of H_2DTG- and ouabain-sensitive current in a single axon. Closed symbols plot the (100 μM) H_2DTG difference I-V relationship corrected for baseline drift. After a 45-min washout, the procedure was repeated with 100 μM ouabain. Open symbols plot the ouabain difference I-V relationship corrected for baseline drift. In both instances, the baseline drift corrections were smaller than the size of the symbols used in the graph. The voltage ranged from −95 to +35 mV in H_2DTG, but from −80 to +20 mV in ouabain because the intervening increase in leak conductance limited the useful range of membrane voltages. Temperature: (A) 17.8–17.9°C; (B) 17.4–17.8°C; (C) 17.8°C.

baseline drift estimates. Fig. 6 B shows the analogous data for ouabain, also simply averaged, obtained from four axons. There are no obvious differences between the two sets except perhaps for the small outward current at positive potentials in the case of H_2DTG.

Since ouabain binds irreversibly to the Na pump of squid giant axons, measurements of ouabain-sensitive difference currents were usually performed after some other protocol(s) had been completed. At the concentration of the reversible blocker H_2DTG used (100 μM), and under our experimental conditions, its difference signal should be ~94% of that of ouabain (Rakowski et al., 1989). To test for a possible difference between the H_2DTG and ouabain results, we measured H_2DTG-sensitive current and then ouabain-sensitive current 1 h later on the same axon (Fig. 6 C). Corrections for baseline drift were very small in both cases (not exceeding the size of the symbols in the case of H_2DTG, or half their size in the case of ouabain), and were applied to the raw difference plots to yield the drift-corrected H_2DTG- or ouabain-sensitive I-V relationships plotted in Fig. 6 C. These appear entirely superimposable. It is likely that the expected minor effect of incomplete inhibition by H_2DTG was approximately offset by a small degree of rundown before the test with ouabain.

Influence of Extracellular [Na^+] on the Backward-running Sodium Pump I-V Curve

The saturating sigmoid shape of the reverse pump I-V relationship, tending to a constant maximal reverse pump current I_{pump}^{max} at extreme negative potentials, is predicted by our model (see DISCUSSION) which features an external high field access/release channel. A key property of the access channel models is that alterations in membrane potential and alterations in concentration of a charged reagent (here, external Na^+) are kinetically equivalent (Mitchell, 1969). Because hyperpolarization enhances the probability (via a Boltzmann partition effect) of extracellular Na^+ ions finding their way to the bottom of the access channel, a reduction of $[Na^+]_o$ is expected to cause a simple leftward displacement of the I-V curve, whereas raising $[Na^+]_o$ should cause a parallel shift toward positive potentials. Conversely, sufficient hyperpolarization (subject to experimental range limitations) should cause saturation of Na-dependent steps at any finite $[Na^+]_o$. In the absence of other major voltage sensitive steps in the reaction cycle, all inward pump I-V curves should reach the same maximum I_{pump}^{max}, regardless of $[Na^+]_o$, at extreme negative membrane potentials where the reverse transport cycle becomes rate-limited by steps independent of voltage and external Na.

These predictions were verified by our findings. First (data not shown), when repeated inward pump I-V curves were obtained on a single axon and fit with Boltzmann partition functions, the (extrapolated) maximal pump current magnitudes I_{pump}^{max} were indistinguishable (except for exponential rundown) whether the axon, if hypertonic, was bathed in 800, 400, or 200 mM Na_o or, if normotonic, in 400 or 200 mM Na_o. Second, Fig. 7 shows that, for both normal tonicity solutions (in which $[Na^+]_o$ of 400 and 200 mM can be compared; Fig. 7 A) and hypertonic solutions (that permit raising $[Na^+]_o$ to 800 mM; Fig. 7 B), the parallel shifts are identical (29 mV) for each twofold change of external Na^+ concentration. The magnitude of this shift reflects the fraction of the membrane's electric field dropped along the postulated access channel, $\lambda = 0.61 \pm 0.03$ (see DISCUSSION). The uniform apparent valence ($z = n\lambda = 0.80$) of all five Boltzmann partition curves reflects, besides the common λ already mentioned, a common molecularity (Hill coefficient) value of $n = 1.33 \pm 0.05$. The midpoint voltages of the curves reflect values for the apparent Na_o affinity in the absence of transmembrane potential ($K_{0.5}^0$) of 715 ± 37 mM for normotonic, and 1,065 ± 80 mM for hypertonic axons.

In practice, the simultaneous global fit to all the data (normotonic and hypertonic) shown in Fig. 7 was pre-

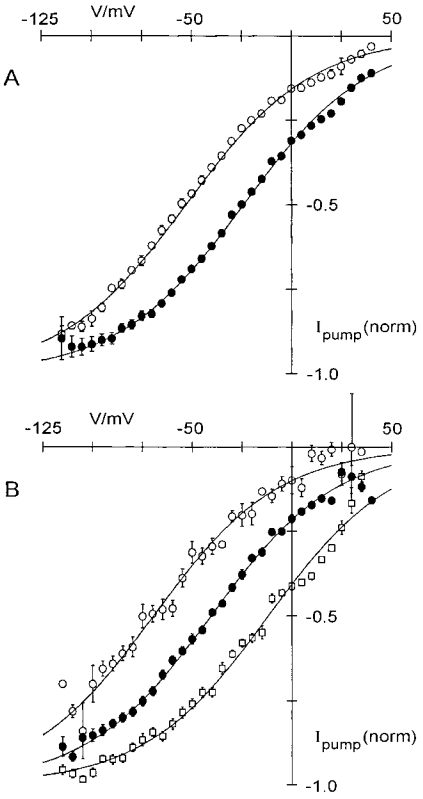

FIGURE 7. Identical shifts of the normalized I-V relationship of the backward-running Na/K pump produced by doubling of $[Na^+]_o$. (A) Mean values of normalized H_2DTG-sensitive current measured in solutions of normal tonicity at 200 (open circles) and 400 mM (closed circles) Na^+_o. The midpoint voltages are −53 and −24 mV, respectively. The number of I-V curves/axons examined for each data set was 5/3 and 9/4, respectively. (B) Mean values of normalized H_2DTG-sensitive current measured in hypertonic seawater containing 200 mM (open circles), 400 mM (closed circles), or 800 mM (open squares) Na^+_o. The midpoint voltages are −70, −41, and −12 mV, respectively. The number of I-V curves/axons examined for each data set was 3/3, 12/8, and 10/6, respectively. All five Boltzmann functions $I_{pump}(norm) = -1/(1 + \exp[(V_m - \bar{V})\, zF/RT])$ are identical in shape with apparent valence z = 0.80 and midpoint voltages $\bar{V}$ as stated. Hypertonicity alone causes a 17-mV leftward shift. The relationship between apparent valence and the shift produced by doubling $[Na^+]_o$ is discussed in the text.

ceded by one (not shown) in which normotonic and hypertonic data were fit separately. After verifying that the refined least-squares parameters did not differ significantly between the two groups, we proceeded with the global fit as described in MATERIALS AND METHODS.

DISCUSSION

Reversal of the Na/K Pump

Garrahan and Glynn (1967) demonstrated enhanced incorporation of $^{32}P_i$ into ATP in resealed red cell ghosts under conditions where reversal of the Na/K pump is expected. Net ATP synthesis was later demonstrated in guinea pig red blood cells (Lew et al., 1970) as well as in rabbit nonmyelinated nerve fibers (Chmouliovsky, 1970). De Weer and Rakowski (1984) showed that, under conditions designed to support reverse pumping in voltage-clamped internally dialyzed squid giant axons, the pump generates inward current. As in cardiac myocytes (Bahinski et al., 1988) and *Xenopus* oocytes (Efthymiadis and Schwarz, 1991), the current-voltage relationship of the backward-running pump is a monotonic function with a positive slope that tends towards saturation (at least for squid axons and guinea pig myocytes) at the negative, and towards zero at the positive, extremes of the experimentally accessible voltage range. Here, we extend these findings to include the influence of external $[Na^+]$, and propose an economical model to account for the pump's steady-state voltage dependence in this and other transport modes.

Reliability of Reverse Pump Current Measurements

The technical difficulties of accurately measuring the small inward current and K^+ efflux generated by the backward-running Na/K pump have been largely overcome. During reverse pumping, K ions are extruded into an extracellular restricted-diffusion space (Frankenhaeuser and Hodgkin, 1956) in which they might support currents not intrinsic to the pump. The control measurements shown in Fig. 5 C set an upper limit to the magnitude of spurious current contributions caused by any changes in $[K^+]_o$ that might occur upon stopping and starting the pump. An independent measure of the reliability of the current measurement is afforded by experiments like that of Fig. 1. Assuming a reverse cycle transport stoichiometry of 2 K ions per elementary charge transferred, a ratio of H_2DTG- or ouabain-sensitive $^{42}K^+$ efflux to current (scaled by Faraday's constant) of 2.0 is expected. We found a ratio of 1.5 ± 0.4, which is not significantly different from the theoretical value. However, the result shows the large residual variability in these difficult simultaneous measurements.

Kinetic Model of the Na/K Pump

The kinetics of the Na/K pump are well described by the Albers-Post model (Albers, 1967; Post et al., 1969; Karlish et al., 1978; Heyse et al., 1994), an outline of which is shown in Fig. 8. In this model, the Na/K pump protein cycles through four major stages, with interlocking alternations of conformation (E_1 versus E_2), and of phosphorylation/dephosphorylation and ion binding/occlusion and deocclusion/release steps. Although these ion binding/release events in reality are composed of successive reactions involving 3 Na or 2 K ions (Fig. 8, boxed area), the steady-state kinetics of each sequence of events are adequately described by the Hill approximation with a single apparent molecularity (n) per sequence. Furthermore, in the experiments described

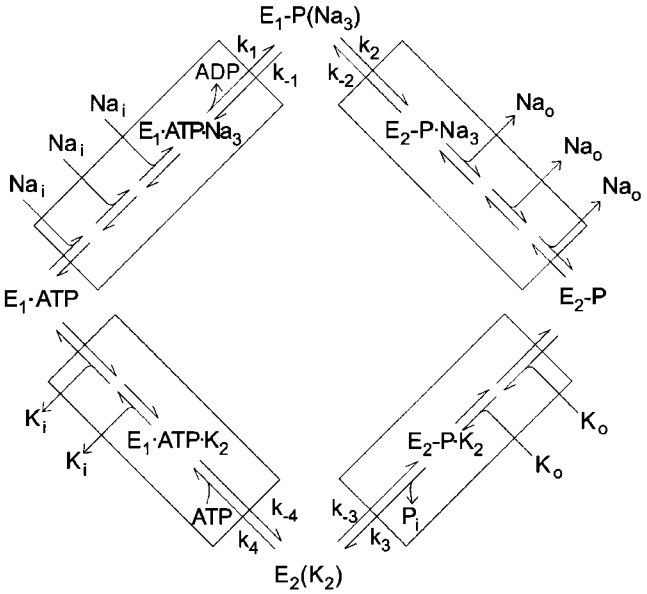

FIGURE 8. Albers-Post kinetic scheme for the sodium pump. Cycle steps are grouped into four ion occlusion or deocclusion reactions: (1) binding and occlusion of three intracellular Na ions, and concomitant phosphorylation of E_1 and release of ADP, with lumped rate coefficients k_1 and k_{-1}; (2) deocclusion of 3 Na ions to the outside as E_1-P undergoes a conformational change to E_2-P, with lumped rate coefficients k_2 and k_{-2}; (3) binding and occlusion of two extracellular K ions, and concomitant dephosphorylation of E_2, with lumped rate coefficients k_3 and k_{-3}; and (4) deocclusion of K^+ as E_2 is converted back to E_1 in a process accelerated by ATP, with lumped rate coefficients k_4 and k_{-4}.

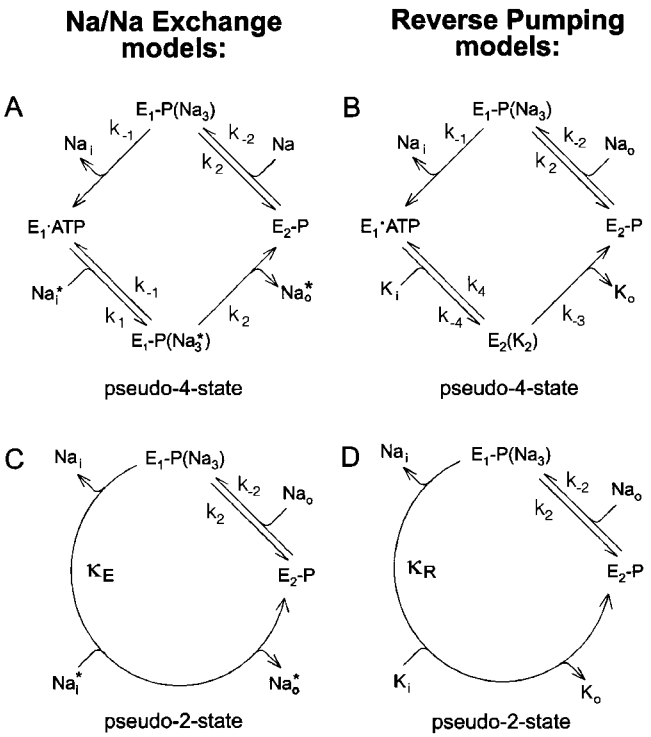

FIGURE 9. Reduced kinetic schemes, derived from that in Fig. 8, for two specific modes of operation of the pump. (A) Pseudo-4-state model for Na/Na* (isotopic) exchange. Note that identical rate coefficients appear in both hemicycles. (B) Pseudo-4-state model for reverse pumping. Note by comparison with Fig. 8 that the pseudo-first-order rate coefficients k_1 and k_3 have been dropped since $[Na^+]_i$ and $[K^+]_o$ were nominally zero in the experiments. Note also that k_2 and k_{-2} in the top hemicycle are identical to those in A. (C) Pseudo-2-state model for Na/Na* exchange, derived from A by lumping all reaction steps but Na^+ deocclusion/reocclusion. (D) Pseudo-2-state model for reverse pumping, derived from B by lumping all reaction steps but Na^+ deocclusion/reocclusion.

here and in our study of Na^+/Na^+ exchange (Gadsby et al., 1993), the intracellular concentrations of ATP, ADP, and P_i were all held approximately constant. For the present discussion of steady-state behavior, the Albers-Post scheme of Fig. 8, therefore, can be compressed (Fig. 9 B) without loss of generality by combining several steps and states (those within the boxes of Fig. 8) into apparent single binding/occlusion and deocclusion/release reactions, with corresponding "lumped" rate constants (Figs. 8 and 9 B) that are either first-order (k_{-1}, k_2, k_{-3}, and k_4) or pseudo-first-order (k_1, k_{-2}, k_3, and k_{-4}). Models derived from steady-state experiments cannot predict presteady-state behavior; in particular, they do not assign voltage sensitivity to individual steps within a lumped group. Presteady-state voltage-jump experiments (Nakao and Gadsby, 1986; Bahinski et al., 1988; Rakowski, 1993; Hilgemann, 1994; Wuddel and Apell, 1995; Peluffo and Berlin, 1997; Holmgren et al., 2000) are needed to resolve demonstrably voltage-sensitive lumped steady-state rate coefficients (such as k_{-2} or k_3) into their component parts. Conversely, kinetic models derived from presteady-state experiments are necessarily constrained by such steady-state observations as reported here.

It is firmly established that positive charge is carried outward across the membrane during the Na^+-translocating part of the forward Na/K pump cycle, predominantly in steps that occur late in the Na^+ hemicycle (for reviews see De Weer et al., 1988, 2000; Läuger, 1991a,b; Rakowski et al., 1997b). Modest voltage dependence of intracellular Na^+ binding also has been shown (Goldshlegger et al., 1987; Stürmer et al., 1991; Heyse et al., 1994; Wuddel and Apell, 1995) but must have contributed little in our experiments both on Na/Na exchange (Gadsby et al., 1993) with $[Na^+]_i$ near-saturating and on reverse pumping, reported here, with $[Na^+]_i$ nominally zero. In the case of the K^+ hemicycle, the apparent affinity of the forward-running pump for K^+ is voltage dependent in *Xenopus* oocytes (Rakowski et al., 1991; Sagar and Rakowski, 1994), cardiac myocytes (Bielen et al., 1991, 1993; Gadsby et al., 1992; Berlin and Peluffo, 1997), and squid giant axons (Rakowski et al., 1997a), and evidence for charge transfer accompanying K^+ binding/occlusion has been ob-

tained (Stürmer et al., 1991; Berlin and Peluffo, 1997; Hilgemann, 1997; Peluffo and Berlin, 1997), with kinetics that suggest that external K^+ access to the pump occurs across a small fraction of the transmembrane electric field. Both our Na/Na experiments (Gadsby et al., 1993) and the present reverse pumping experiments were carried out in K^+_o-free conditions.

Two Modes: Na^+/Na^+ Exchange and Reverse Pumping

Because the ADP-requiring Na^+/Na^+ exchange mode and the reverse pumping mode likely have reaction steps in common, and because we have identified (Gadsby et al., 1993) a putative step in the steady-state model that renders the Na^+/Na^+ exchange mode voltage sensitive (see also Heyse et al., 1994; Hilgemann, 1994; Wuddel and Apell, 1995; Holmgren et al., 2000), it is instructive to compare the pseudo-4-state schemes appropriate for these two modes (Fig. 9). In the Na^+/Na^+ exchange mode (Fig. 9 A), the enzyme is constrained to oscillate within the Na^+ hemicycle, alternately transporting labeled Na^+ outward and unlabeled Na^+ inward over the same pathway. Hence, of the eight rate coefficients from the full cycle Albers-Post model of Fig. 8, only four (three of them independent because of the microscopic reversibility constraint) are needed to describe the four-step Na^+/Na^+ exchange mode. Moreover, because only the internal solution contains labeled Na^+, external release of labeled Na^+ and internal release of unlabeled Na^+ are effectively irreversible steps, each governed by a rate coefficient (k_2 and k_{-1}, respectively) that also affects another, reversible, step in the cycle. In the reverse pumping mode (Fig. 9 B), the enzyme traverses all four pseudosteps of the full Albers-Post cycle but, because our zero-trans (Na^+- and K^+-free) experimental conditions render two of the four steps irreversible, two rate coefficients of the full model (k_1 and k_3; Fig. 8) vanish. Comparison of Fig. 9, A and B, and of the contents of our external solutions shows that when $[Na^+]_o$ is the same, the two models share rate coefficients k_2 and k_{-2} (though probably not k_{-1} because somewhat different ADP concentrations were used in the two types of experiment).

Voltage Dependence of Na^+/Na^+ exchange

In the discussion that follows, we will analyze the steady-state voltage dependence of the reverse pumping mode in light of our previous findings on the Na^+/Na^+ exchanging mode. We have shown (Gadsby et al., 1993) that the steady-state rate of electroneutral Na^+/Na^+ exchange (with $[Na^+]_i$ kept high) is enhanced by hyperpolarization along a saturating sigmoid curve which, itself, undergoes identical leftward shifts (without change in shape) for each twofold reduction of $[Na^+]_o$. The observed fixed relationship among (1) the steepness of the fitted Boltzmann distribution equation, (2) the dependence of the sigmoid's midpoint voltage on $[Na^+]_o$, and (3) the Hill coefficient for exchange activation by external Na^+ reflects kinetic equivalence between $[Na^+]_o$ and membrane potential. These relationships compellingly point to the external Na^+ rebinding/occlusion step (pseudo-first-order rate coefficient k_{-2} in Fig. 9 A) as the major rate-limiting voltage-sensitive reaction of the overall steady-state cycle, in the experimentally accessible voltage range. (Under the experimental conditions we used, i.e., $[Na^+]_i \geq 50$ mM, the voltage sensitivity of Na^+_i binding mentioned earlier is negligible for practical purposes). A formal interpretation of the observed behavior is that step 2 takes place over an Eyring barrier that is positioned highly asymmetrically within the membrane electrical field (our data required ≥95% asymmetry; see Gadsby et al., 1993). Models with a symmetric Eyring barrier in step 2 require additional particular relationships among the four (or three independent) rate coefficients to fit the data (see below). The most parsimonious, and physically appealing interpretation (Gadsby et al., 1993) of the observed behavior is that all rate coefficients of the simplified scheme of Fig. 9 A, including the intrinsic higher-order rate coefficient k_2, are effectively voltage independent under the prevailing experimental conditions, whereas Na^+ binding occurs at the bottom of a high field access channel, i.e., within the membrane electric field, so that the probability of Na ions reaching their binding site becomes an exponential function of membrane potential. (The escape rate of ions from the channel is similarly governed by V_m but, since it is expected to be orders of magnitude faster than the rate-limiting enzymatic deocclusion step(s), it should have no perceptible effect on overall steady-state cycling rate.) Consequently the expression for the pseudo-first-order rate coefficient k_{-2} becomes an exponential function of V_m:

$$k_{-2} = k'_{-2}\left[[Na^+]_o \exp\left(\frac{-\lambda V_m F}{RT}\right)\right]^n, \qquad (1)$$

where k'_{-2} is the corresponding voltage-insensitive intrinsic higher-order rate coefficient, λ is the fraction of the membrane field dropped along the access channel measured from the external solution edge, and n is the empirical Hill coefficient (apparent molecularity) of external Na^+ binding. In this simple physical model, the lateral voltage shifts caused by doubling of $[Na^+]_o$ are defined by $\Delta V = (RT/\lambda F)\ln 2$, and the apparent valence of the Boltzmann partition function is defined as $z = n\lambda$.

If k_{-2} is effectively (over the accessible voltage range) the sole voltage sensitive rate coefficient in the Na^+/Na^+ exchange reaction scheme of Fig. 9 A, then this pseudo-4-state scheme may be further reduced to the pseudo-2-state Na^+/Na^+ exchange scheme of Fig. 9 C, without loss of kinetic information with regard to

steady-state dependence of exchange rate on V_m and $[Na^+]_o$. (For a general proof that any multistep unbranched reaction cycle with a single voltage-sensitive step can be reduced to a pseudo-two-state model for the purpose of describing the voltage sensitivity of steady-state currents or turnover rates see Hansen et al., 1981.) Indeed, standard derivation methods (King and Altman, 1956) applied to either the pseudo-four-state or the pseudo-two-state model yield identical kinetic expressions for the exchange flux rate $\Phi_{Na/Na} = f([Na^+]_o)$ $K_{0.5}$ or $\Phi_{Na/Na} = f(V_m)$:

$$\Phi_{NaNa} = \frac{\Phi_{NaNa}^{max}}{1 + \left[\frac{K_{0.5}^0 \exp\left(\frac{\lambda V_m F}{RT}\right)}{[Na^+]_o}\right]^n}, \quad (2a)$$

(a Hill equation with voltage-sensitive apparent $K_{0.5}$), or

$$\Phi_{NaNa} = \frac{\Phi_{NaNa}^{max}}{1 + \exp\left[\frac{(V_m - \bar{V})n\lambda F}{RT}\right]}, \quad (2b)$$

(a Boltzmann equation with $[Na^+]_o$-dependent midpoint), where $\bar{V}$ (the midpoint voltage of the Boltzmann equation) and $K_{0.5}^0$ (the Na^+ concentration for half-maximal exchange flux activation at $V_m = 0$) are related by

$$\bar{V} = \frac{RT}{\lambda F} \ln \frac{[Na^+]_o}{K_{0.5}^0}.$$

In terms of the models' rate coefficients, the Na^+ concentration for half-maximal activation of Na^+/Na^+ exchange rate $\Phi_{Na/Na}$ at $V_m = 0$ is given by:

$$K_{0.5}^0 = \left[\frac{k_2}{k_{-2}\left(1 + \frac{k_{-1}}{k_1}\right)}\right]^{1/n},$$

for the pseudo-4-state model (Fig. 9 A), or

$$K_{0.5}^0 = \left[\frac{k_2 + \kappa_E}{k_{-2}}\right]^{1/n},$$

for the pseudo-2-state model (Fig. 9 C), where κ_E is a lumped (apparent) rate constant governing all reaction steps of the exchange cycle except for the external Na^+ binding/occlusion and deocclusion/release steps.

Voltage Dependence of Reverse Pumping

A corollary of the compelling evidence, just discussed, for voltage dependence of rate coefficient k_{-2} is that this same rate coefficient, since it figures in the pseudo-4-state reverse pump reaction scheme of Fig. 9 B, may contribute to the voltage dependence of the reverse pumping mode as well. Our findings reported here show that the voltage dependence of reverse pumping is well described by the simplest (i.e., high field access channel) model that accounts for the Na^+/Na^+ exchange kinetics, with rate expressions entirely analogous to Eqs. 2a and 2b. In fact (data not shown), we were able to satisfactorily fit simultaneously both Na^+/Na^+ exchange (data of Gadsby et al., 1993) and reverse pumping data with a single set of values for λ (fraction of membrane field traversed by external Na^+ ions within the access channel), apparent molecularity or Hill coefficient (n) and, hence, apparent valence ($z = n\lambda$).

If k_{-2} is, for practical purposes, the sole voltage-sensitive rate coefficient in the pseudo-4-state reverse pumping scheme of Fig. 9 B by virtue of a high field access channel effect (Eq. 1), then that scheme too can be reduced to a pseudo-2-state model (Fig. 9 D). Accordingly, the backward-running pump appears to operate in two steps (a and b). One of these is Na^+- and voltage-sensitive because it includes the binding of (at least one) Na^+ by a voltage-sensitive mechanism; the other reflects all remaining reactions in the reverse pump cycle. The general expression for the cycling rate, $a \cdot b/(a + b)$, can be cast in two forms (Eq. 3, a and b)

$$I_{pump} = \frac{I_{pump}^{max}}{1 + \left(\frac{K_{0.5}^0 \exp\left(\frac{\lambda V_m F}{RT}\right)}{[Na^+]_o}\right)^n}, \quad (3a)$$

(a Hill equation with voltage-sensitive apparent $K_{0.5}$), or

$$I_{pump} = \frac{I_{pump}^{max}}{1 + \exp\left[\frac{(V_m - \bar{V})n\lambda F}{RT}\right]}, \quad (3b)$$

(a Boltzmann equation with $[Na^+]_o$-dependent midpoint), which are identical to those given above (Eq. 2, a and b) for the rate of Na^+/Na^+ exchange $\Phi_{Na/Na}$ except, naturally, for the components of $K_{0.5}^0$ for Na^+ (pseudo-4-state model; Fig. 9 B):

$$K_{0.5}^0 = \left[\frac{k_{-3}k_{-4}(k_{-1} + k_2)}{k_{-2}(k_{-1}[k_{-3} + k_4] + k_{-4}[k_{-1} + k_{-3}])}\right]^{1/n},$$

or (pseudo-2-state model; Fig. 9 D):

$$K_{0.5}^0 = \left[\frac{k_2 + \kappa_R}{k_{-2}}\right]^{1/n},$$

where κ_R is a lumped (apparent) rate constant governing all reaction steps of the backward pumping cycle except for the external Na^+ binding/occlusion and deocclusion/release steps. As shown earlier, the characteristic sensitivity of the reverse pump to V_m and $[Na^+]_o$ (data of Fig. 7) is well described by this parsimonious

model. The model's merit over more complex ones is its ability to equally account for the kinetics of voltage and Na^+ dependence of two modes of operation of the sodium pump (electroneutral Na^+/Na^+ exchange and reverse pumping) without further assumptions.

Kinetic expressions for more elaborate models of Na^+/Na^+ exchange also reduce to those derived for the access channel model, provided certain constraints on the individual rate coefficients are satisfied. For example, if both k_2 and k_{-2} in the pseudo-4-state scheme of Fig. 8 were voltage-sensitive rate coefficients by virtue of a symmetric Eyring barrier in step 2 (i.e., Na^+ deocclusion/release or rebinding/occlusion), the resulting kinetic expressions would be more complex, not only for pump current I_{pump} in the reverse mode (Fig. 9 B), but especially for the flux rate $\Phi_{Na/Na}$ in the Na^+/Na^+ exchange mode (Fig. 9 A) because the reciprocating character of the latter causes rate coefficient k_2 to govern two of the four steps in the cycle. Specifically, the I_{pump}-V and $\Phi_{Na/Na}$-V curves are no longer simple Boltzmann partition functions; the lateral shifts with changes in $[Na^+]_o$ are not identical for I_{pump}-V and $\Phi_{Na/Na}$-V curves, nor are they uniform for each doubling of $[Na^+]_o$; the steepness of the curves is not uniform; and the $\Phi_{Na/Na}$-V curves at various $[Na^+]_o$ do not tend to the same $\Phi_{Na/Na}$. Given certain constraints on the relationships between individual rate coefficients, these complex equations for the Eyring barrier model can be made to formally approximate those for the high field access model and satisfy some, but not all, of its criteria. For example, if $k_{-1} \ll k_{-2}$, then each doubling of $[Na^+]_o$ will cause uniform parallel shifts (i.e., the curves will retain their slopes as they move sideways a fixed distance), but the magnitudes of the lateral shifts will differ between I_{pump}-V and $\Phi_{Na/Na}$-V curves, and the slope of the curves will differ for the two modes. We found no model with an Eyring barrier in step 2, whether symmetric (Läuger and Stark, 1970) or with <90% asymmetry, that gave a satisfactory simultaneous fit to both Na^+/Na^+ exchange and reverse pumping data.

Comparison of A and B in Fig. 9 now raises the question whether the rate coefficient k_{-3} (Fig. 9 B) could have a characteristic voltage dependence sufficiently similar to that of k_2 (which occupies an analogous position in the isotope hemicycle of Na^+/Na^+ exchange, see Fig. 9 A) to endow the reverse pumping cycle with a voltage sensitivity formally indistinguishable from that of the Na^+/Na^+ exchange mode. This possibility is remote for two reasons. First, the voltage sensitivity of the K^+ hemicycle is known to be much weaker than that of the Na^+ hemicycle (Bielen et al., 1991, 1993; Rakowski et al., 1991; Stürmer et al., 1991; Gadsby et al., 1992; Sagar and Rakowski, 1994; Bühler and Apell, 1995; Berlin and Peluffo, 1997; Hilgemann, 1997; Peluffo and Berlin, 1997; Rakowski et al., 1997a). Second, if the weak voltage dependence of step 3 (in the pseudo-4-state model of Fig. 8) is ascribed to a high field access channel mechanism (Sagar and Rakowski, 1994; Bühler and Apell, 1995; Berlin and Peluffo, 1997; Peluffo and Berlin, 1997; Rakowski et al., 1997a), then the intrinsic first-order rate coefficient k_{-3} will be devoid of voltage sensitivity.

The average maximum inward pump current we observed in this study was roughly one third to one half as large as the maximum forward Na^+/K^+ transport current we observed previously in squid giant axon (Rakowski et al., 1989). Since $^{22}Na^+$ efflux in the Na^+/Na^+ exchange mode (Gadsby et al., 1993) represents an approximately similar fraction of the $^{22}Na^+$ efflux mediated by forward pumping, we surmise that the electroneutral Na^+/Na^+ exchange and reverse transport modes are rate-limited by a common voltage-independent transition, perhaps within step 1 of the pseudo-4-step Albers-Post model (Fig. 8).

Influence of Hypertonic Solutions

Fig. 7 shows that hypertonic solutions do not modify the least-squares fit values of the fractional electrical distance (λ) or the apparent molecularity (Hill coefficient n) of our access channel model. However, they do reduce the apparent affinity for Na^+ ~1.5-fold: $K^0_{0.5}$ is 715 ± 37 mM in normotonic solutions (Fig. 7 A), but 1,065 ± 80 mM in hypertonic solutions (Fig. 7 B). This causes a uniform 17-mV leftward shift of the Boltzmann partition curves of Fig. 7 B compared with those of Fig. 7 A. To examine whether this could be due to additional shielding of negative membrane surface charges by the high ionic strength seawater, we used the Grahame (1947) equation and found that no more than about 1/3 of the observed shift could be ascribed to additional shielding by the hypertonic seawater. Therefore, other mechanisms (e.g., anion effects; Suzuki and Post, 1997) must (also) come into play to lower the apparent affinity for Na^+ in hypertonic seawater.

Conclusion

The extracellular Na^+ access channel model we proposed for the voltage dependence of the steady-state rate of electroneutral Na^+/Na^+ exchange (Gadsby et al., 1993) is strongly supported by our finding here that, formally, it accounts equally well and without additional postulates for the voltage dependence of the steady-state rate of reverse electrogenic pumping. Assuming structural homology between Ca-ATPase and Na,K-ATPase, it is also compatible with the structure of the sarcoplasmic reticulum calcium pump published by Toyoshima et al. (2000), which features Ca^{2+} binding/release sites deep inside the protein, near the cytosolic end of its transmembrane domain. More complex models that account for the steady-state voltage dependence of Na^+/Na^+ exchange, such as those featuring symmetric Eyring barriers, cannot be constrained to ac-

commodate all of the features of the steady state voltage dependence of reverse pumping as well unless demonstrably implausible assumptions (e.g., strong voltage dependence in the K^+ hemicycle) are included. These requirements render alternative models highly contrived and, therefore, less likely.

This research was supported by National Institutes of Health grants NS11223 (to P. De Weer), NS22979 (to D.C. Gadsby), and HL36783 (to R.F. Rakowski).

Submitted: 4 August 2000
Revised: 16 January 2001
Accepted: 6 February 2001

REFERENCES

Albers, R.W. 1967. Biochemical aspects of active transport. *Annu. Rev. Biochem.* 36:727–756.

Apell, H.-J. 1989. Electrogenic properties of the Na,K pump. *J. Membr. Biol.* 110:103–114.

Argüello, J.M., R.D. Peluffo, J. Feng, J.B. Lingrel, and J.R. Berlin. 1996. Substitution of glutamic 779 with alanine in the Na,K-ATPase α subunit removes voltage dependence of ion transport. *J. Biol. Chem.* 271:24610–24616.

Axelsen, K.B., and M.G. Palmgren. 1998. Evolution of substrate specificities in the P-type ATPase superfamily. *J. Mol. Evol.* 46:84–101.

Bahinski, A., M. Nakao, and D.C. Gadsby. 1988. Potassium translocation by the Na/K pump is voltage insensitive. *Proc. Natl. Acad. Sci. USA.* 85:3412–3416.

Berlin, J.R., and R.D. Peluffo. 1997. Mechanism of electrogenic reaction steps during K^+ transport by the Na,K-ATPase. *Ann. NY Acad. Sci.* 834:251–259

Bielen, F.V., H.G. Glitsch, and F. Verdonck. 1991. Dependence of Na^+ pump current on external monovalent cations and membrane potential in rabbit cardiac Purkinje cells. *J. Physiol.* 442: 169–189.

Bielen, F.V., H.G. Glitsch, and F. Verdonck. 1993. Na^+ pump current-voltage relationships of rabbit cardiac Purkinje cells in Na^+-free solution. *J. Physiol.* 465:699–714.

Bühler, R., and H.-J. Apell. 1995. Sequential potassium binding at the extracellular side of the Na,K-pump. *J. Membr. Biol.* 145:165–173

Chmouliovsky, M. 1970. Synthesis of ATP by reversal of the Na/K pump in rabbit non-myelinated nerve fibres. *Experientia.* 26:679.

De Weer, P., and R.F. Rakowski. 1984. Current generated by backward-running electrogenic Na pump in squid giant axons. *Nature.* 309:450–452.

De Weer, P., D.C. Gadsby, and R.F. Rakowski. 1988. Voltage dependence of the Na-K pump. *Annu Rev. Physiol.* 50:225–241.

De Weer, P., D.C. Gadsby, and R.F. Rakowski. 2000. The Na/K-ATPase: a current-generating enzyme. *In* Na/K-ATPase and Related ATPases. K. Taniguchi and S. Kaya, editors. Elsevier Science Publishing Co., Inc., NY. 27–34.

Di Polo, R., L. Beaugé. 1987. Characterization of the reverse Na/Ca exchange in squid axons and its modulation by Ca_i and ATP. Ca_i-dependent Na_i/Ca_o and Na_i/Na_o exchange modes. *J. Gen. Physiol.* 90:505–525.

Efthymiadis, A., and W. Schwarz. 1991. Conditions for backward-running Na^+/K^+ pump in *Xenopus* oocytes. *Biochim. Biophys. Acta.* 1068:73–76.

Frankenhaeuser, B., and A.L. Hodgkin. 1956. The after-effects of impulses in the giant nerve fibres of *Loligo. J. Physiol.* 116:449–472.

Gadsby, D.C., and M. Nakao. 1989. Steady-state current-voltage relationship of the Na/K pump in guinea pig ventricular myocytes. *J. Gen. Physiol.* 94:511–537.

Gadsby, D.C., J. Kimura, and A. Noma. 1985. Voltage dependence of Na/K pump current in isolated heart cells. *Nature.* 315:63–65.

Gadsby, D.C., M. Nakao, A. Bahinski, G. Nagel, and M. Suenson. 1992. Charge movements via the cardiac Na,K-ATPase. *Acta Physiol. Scand.* 146:111–123.

Gadsby, D.C., R.F. Rakowski, and P. De Weer. 1993. Extracellular access to the Na,K pump: pathway similar to ion channel. *Science.* 260:100–103.

Garrahan, P.J., and I.M. Glynn. 1967. The incorporation of inorganic phosphate into adenosine triphosphate by reversal of the sodium pump. *J. Physiol.* 192:237–256.

Glitsch, H.G., T. Krahn, and H. Pusch. 1989. The dependence of sodium pump current on internal Na concentration and membrane potential in cardioballs from sheep Purkinje fibres. *Pflügers Archiv.* 414:52-58.

Goldshlegger, R., S.J.D. Karlish, A. Rephaeli, and W.D. Stein. 1987. The effect of membrane potential on the mammalian sodium-potassium pump reconstituted into phospholipid vesicles. *J. Physiol.* 387:331–355.

Grahame, D.C. 1947. The electrical double layer and the theory of electrocapillarity. *Chem. Rev.* 41:441–501.

Hansen, U.-P., D. Gradmann, D. Sanders, and C.F. Slayman. 1981. Interpretation of current-voltage relationships for "active" ion transport systems: I. Steady-state reaction-kinetic analysis of class-I mechanisms. *J. Membr. Biol.* 63:165–190.

Heyse, S., I. Wuddel, H.-J. Apell, and W. Stürmer. 1994. Partial reactions of the Na, K-ATPase: determination of rate constants. *J. Gen. Physiol.* 104:197–240.

Hilgemann, D.W. 1994. Channel-like function of the Na,K pump probed at microsecond resolution in giant membrane patches. *Science.* 263:1429–1432.

Hilgemann, D.W. 1997. Recent electrical snapshots of the cardiac Na,K pump. *Ann. NY Acad. Sci.* 834:260–269.

Holmgren, M., J. Wagg, F. Bezanilla, R.F. Rakowski, P. De Weer, and D.C. Gadsby. 2000. Three distinct and sequential steps in the release of sodium ions by the Na^+/K^+-ATPase. *Nature.* 403:898–901.

Horisberger, J.-D., P. Jaunin, P.J. Good, B.C. Rossier, and K. Geering. 1991. Coexpression of α_1 with putative β_3 subunits results in functional Na^+/K^+ pumps in *Xenopus* oocytes. *Proc. Natl. Acad. Sci. USA.* 88:8397–8400.

Karlish, S.J.D., D.W. Yates, and I.M. Glynn. 1978. Conformational transitions between Na^+-bound and K^+-bound forms of (Na^+ + K^+)-ATPase studied with formycin nucleotides. *Biochim. Biophys. Acta.* 525:252–264.

King, E.L., and C. Altman. 1956. A schematic method of deriving the rate laws for enzyme-catalyzed reactions. *J. Phys. Chem.* 60: 1375–1378.

Kockskämper, J., G. Gisselmann, and H.G. Glitsch. 1997. Comparison of ouabain-sensitive and -insensitive Na/K pumps in HEK293 cells. *Biochim. Biophys. Acta.* 1325:197–208.

Lafaire, A.V., and W. Schwarz. 1986. Voltage dependence of the rheogenic Na^+/K^+ ATPase in the membrane of oocytes of *Xenopus laevis. J. Membr. Biol.* 91:43–51.

Läuger, P. 1991a. Electrogenic Ion Pumps. Sinauer Associates, Inc., Sunderland, MA. 313 pp.

Läuger, P. 1991b. Kinetic basis of voltage dependence of the Na,K pump. *In* The Sodium Pump. Structure, Mechanism and Regulation. J. Kaplan and P. De Weer, editors. Society of General Physiologists Series. Vol 46. Rockefeller University Press, NY. 303–315.

Läuger, P., and G. Stark. 1970. Kinetics of carrier-mediated ion transport across lipid bilayer membranes. *Biochim. Biophys Acta.* 211:458–466.

Lew, V.L., I.M. Glynn, and J.C. Ellory. 1970. Net synthesis of ATP by reversal of the sodium pump. *Nature.* 225:865–866.

Mitchell, P. 1969. Chemiosmotic coupling and energy transduc-

tion. *Theor. Exp. Biophys.* 2:159–216.

Nakao, M., and D.C. Gadsby. 1986. Voltage dependence of Na translocation by the Na/K pump. *Nature.* 323:628–630.

Nakao, M., and D.C. Gadsby. 1989. [Na] and [K] dependence of the Na/K pump current-voltage relationship in guinea pig ventricular myocytes. *J. Gen. Physiol.* 94:539–565.

Peluffo, R.D., and J.R. Berlin. 1997. Electrogenic K^+ transport by the Na^+-K^+ pump in rat cardiac ventricular myocytes. *J. Physiol.* 501:33–40.

Post, R.L., T. Kume, T. Tobin, B. Orcutt, and A.K. Sen. 1969. Flexibility of an active center in sodium-plus-potassium adenosine triphosphatase. *J. Gen. Physiol.* 54:306–326.

Rakowski, R.F. 1993. Charge movement by the Na/K pump in *Xenopus* oocytes. *J. Gen. Physiol.* 101:117–144.

Rakowski, R.F., and C.L. Paxson. 1988. Voltage dependence of Na/K pump current in *Xenopus* oocytes. *J. Membr. Biol.* 106:173–182.

Rakowski, R.F., D.C. Gadsby, and P. De Weer. 1989. Stoichiometry and voltage dependence of the sodium pump in voltage-clamped, internally dialyzed squid giant axon. *J. Gen. Physiol.* 93:903–941.

Rakowski, R.F., L.A. Vasilets, J. La Tona, and W. Schwarz. 1991. A negative slope in the current-voltage relationship of the Na^+/K^+ pump in *Xenopus* oocytes produced by reduction of external $[K^+]$. *J. Membr. Biol.* 121:177–187.

Rakowski, R.F., F. Bezanilla, P. De Weer, D.C. Gadsby, M. Holmgren, and J. Wagg. 1997a. Charge translocation by the Na/K pump. *Ann. NY Acad. Sci.* 834:231–243.

Rakowski, R.F., D.C. Gadsby, and P. De Weer. 1997b. Voltage dependence of the Na/K pump. *J. Membr. Biol.* 155:105–112.

Sagar, A., and R.F. Rakowski. 1994. Access channel model for the voltage dependence of the forward-running Na^+/K^+ pump. *J. Gen. Physiol.* 103:869–894.

Simchowitz, L., R. Ratzlaff, and P. De Weer. 1986. Anion/anion exchange in human neutrophils. *J. Gen. Physiol.* 88:195–217.

Stürmer, W., H.-J. Apell, I. Wuddel, and P. Läuger. 1989. Conformational transitions and charge translocation by the Na,K Pump: comparison of optical and electrical transients by ATP-concentration jumps. *J. Membr. Biol.* 110:67–86.

Stürmer, W., R. Bühler, H.-J. Apell, and P. Läuger. 1991. Charge translocation by the Na,K-pump: II. Ion binding and release at the extracellular face. *J. Membr. Biol.* 121:163–176.

Suzuki, K., and R.L. Post. 1997. Equilibrium of phosphointermediates of sodium and potassium ion transport adenosine triphosphatase. Action of sodium ion and Hofmeister effect. *J. Gen. Physiol.* 109:537–554.

Toyoshima, C., M. Nakasako, H. Nomura, and H. Ogawa. 2000. Crystal structure of the calcium pump of sarcoplasmic reticulum at 2.6 Å resolution. *Nature.* 405:647–655.

Wuddel, I., and H.-J. Apell. 1995. Electrogenicity of the sodium transport pathway in the Na,K-ATPase probed by charge-pulse experiments. *Biophys. J.* 69:909–921.